This is a post-peer-review, pre-copyedit version of an article published in **IEEE Compatibility in Power Electronics (2005)**. The final authenticated version is available online at: https://doi.org/10.1109/CPE.2005.1547571

MODELING AND EXPERIMENTAL INVESTIGATION OF THE SMALL UPQC SYSTEMS

Ryszard STRZELECKI[*], Grzegorz BENYSEK[**], Jacek RUSIŃSKI[***]

[*]Gdynia Maritime University, Department of Ship Automation
Morska 81-87, 81-225 Gdynia, Poland, e-mail:rstrzele@am.gdynia.pl

[**]University of Zielona Gora, Institute of Electrical Engineering
Podgórna 50, 65-246 Zielona Gora, Poland, e-mail:G.Benysek@iee.uz.zgora.pl

[***]University of Zielona Gora, Institute of Electrical Engineering
Podgórna 50, 65-246 Zielona Gora, Poland, e-mail:J.Rusinski@iee.uz.zgora.pl

Abstract: In this paper the basis of analytical modelling of the UPQC arrangements (Unified Power Quality Conditioner) in d-q rotating coordinates, as well as select results of investigations conducted on the simplified small power laboratory model were talked over. In short form power balance as well as fundamental dependences and analytic model with regard of decoupling circuits were investigated. Applied method for DC link capacity selection was talked over in detail and additionally confirmed with experimental results. Results of simulation and experimental investigations, including operation of the UPQC arrangement in case of burden of the supply with thyristor rectifier were also introduced.

Keywords: Power quality, UPQC, Series-Parallel Active Power Filter, modelling, decupling

The Polish State Committee for Scientific Research,
Project KBN No. 4 T10A 037 25
"Power Electronics Arrangements for Flexible Power Flow Control in Distributed AC Fed Systems",
supported this work.

1. INTRODUCTION

From many years improvement of quality of delivery and receipt of electric energy, is one of the most important areas of application of power electronics arrangements. In this area active power filters (APF) [2, 10,16,25,31,42] occupy significant position. Beginning of them dates year 1976, when appeared many times mentioned [1]. From this moment, literature in this topic is constantly complemented with new positions.

Particularly, increase in number and quality of the papers related to the APF arrangements is possible to observe in last decade of the 20th century. In this period, numerous theoretical studies and application proposals appeared, e.g. [3,5,6,8,9,11,15,19,24]. Also appeared conception described in [4] and another works related to the series-parallel active power filters (S-PAPF) [7,12,13,14,18,21,22,23]. Such arrangements, called also "Unified Power Quality Conditioners" (UPQC) [17], still are subject of the intensive practical investigations and significant scientific publications [27,32,33,36,40]. One can connect this with functional possibilities of them, as well as with development of methods and control algorithms [20,26,28,29,35,37,38, 40,41,42,44]. It should be expected, that in short time UPQC arrangements will find more and more wide, also residential applications [39].

In the following paper there is presented, created with minimum number of simplifying assumptions, UPQC's full model in *d-q* rotating coordinates. This model makes also possible the double "decoupling" of the state-spaces for both passive *LC* filters, those in parallel as well as in series arrangement. It permits to entirely independent control in relation to *p* and *q* coordinates. The double decoupling usually is not proposed and from introduced in [37] differs because of: i) different character of the parallel and series arrangements acting as adding sources; ii) possible simpler realization.

Proposed model is useful in stability investigations, selection of the regulators' parameters as well as values of the passive elements. On this basis, with omission of influence of the fast dynamic processes in *LC* circuits of the adding sources, method for analytic determination of the DC link capacitance, coupling both parallel and series arrangements, was worked out and verified experimentally. Theoretical investigations presented in this paper are also completed with different experimental results, confirming good filtration-compensating proprieties as well as multi-functionality of the UPQC arrangements.

2. SCHEME OF THE INVESTIGATED UPQC

Presented in Fig.1, 3-phase UPQC (Unified Power Quality Conditioner) consists of series (SAPF - Series Active Power Filter) and parallel (PAPF - Parallel Active Power Filter) energetic active filters, joining common DC circuit. SAPF - u'_C voltage source - filtrates harmonics and stabilizes in point of measurement load voltage u_L, during source voltage u_S changes and deformations. PAPF - i'_C current source - compensates passive components in load current i_L. Small filters, L_V–C_V as well as L_I–C_I (alongside with dumping circuits R'_V–C'_V as well as R'_I–C'_I) provide filtration of the harmonics related to PWM control.

The main controller controls U_{DC} voltage and on basis of measured instantaneous i_L, u_S values as well as reference values U^*_{DC} and u^*_L, calculates standard current i^*_C and voltage u^*_C courses. Calculations are realized in d-q coordinates, rotating with frequency $\omega_S=2\pi/T_S$, where: T_S - period of the network voltage. In this case symmetrical components with frequencies ω_S are transferred to 0Hz, what simplifies extraction and regulators of the compensated components. This is also much more easy to control power balance in arrangement. Active power balance unsettling:

$$\int_{t-T_S}^{t} p_V dt = -\int_{t-T_S}^{t} p_I dt \ , \ \int_{t-T_S}^{t} p_S dt = \int_{t-T_S}^{t} p_P dt = \int_{t-T_S}^{t} p_L dt \quad (1)$$

causes U_{DC} voltage changes. To stabilize this voltage, controller forces additional component in i_C current, in phase with u_I voltage. In d-q coordinates most often this is a periodic course.

The d-q coordinates application unfortunately in arrangements with passive elements causes through couplings (look Appendix). In this case simple control in relation to one coordinate, inflict on courses in second coordinate. To eliminate this unfavorable phenomenon, controllers have to realize the "decoupling".

In introduced in Fig.1 UPQC arrangement, with LC filters, one should realize the "double decoupling". Such way of decoupling, explains model discussed in next chapter.

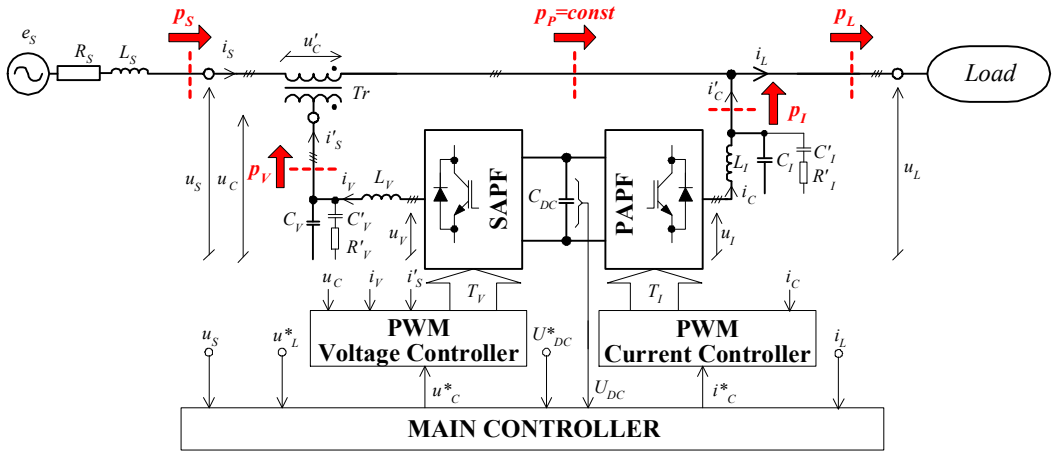

Fig.1. Scheme of the investigated UPQC.

3. MODELING

Models of the individual circuits as well as UPQC full 3-phase model, are elaborated for d-q coordinates with regard to the following assumptions:

- all circuits in UPQC are symmetrical;
- PWM controllers in SAPF and PAPF, do not come into range of over-modulation [28];
- frequency of the triangular carrier in PWM modulator is so large, that in case of L_V–C_V as well as L_I–C_I filters, its influence is negligible;
- pulsations and U_{DC} voltage changes are controlled and do not cause deformations in shaped in closed-loop adding (compensating) currents and voltages;
- the adding transformers' ratio Tr, is set to be 1:1 and additionally there is skipped influence of the main impedance.

Models are introduced below and are only in form of block diagrams, linked undeniably with their mathematical description (look Appendix). Therefore mathematical description in category of state-space equations in d-q and/or α–β coordinates is skipped in this paper.

3.1. Model of the supply line

This model, presented as the block diagram in Fig.2a, considers L_S inductance and supply network resistance R_S as well as losses resistance R_{Tr} and the dispersion inductance L_{Tr} in an adding transformer Tr. One should notice, that in practice short circuit impedance in transformer many times tops network short circuit impedance. Therefore simplified model of the supply line, presented in Fig.2b and further applied in this paper, is sufficiently adequate. Voltage u_S in point of measurement practically is the same as source voltage e_S. Despite of that, in measure arrangement (Fig.3) there is advisable the additional correction of the measured voltage u_S, with consideration of the voltage drop on transformer. Such correction, demands knowledge the transformer's parameters as well as current $i_S = i'_C + i_L \approx i_C + i_L$ – this concerns mostly frequency ω_S. Harmonics in current i_L will be compensated by the PAPF.

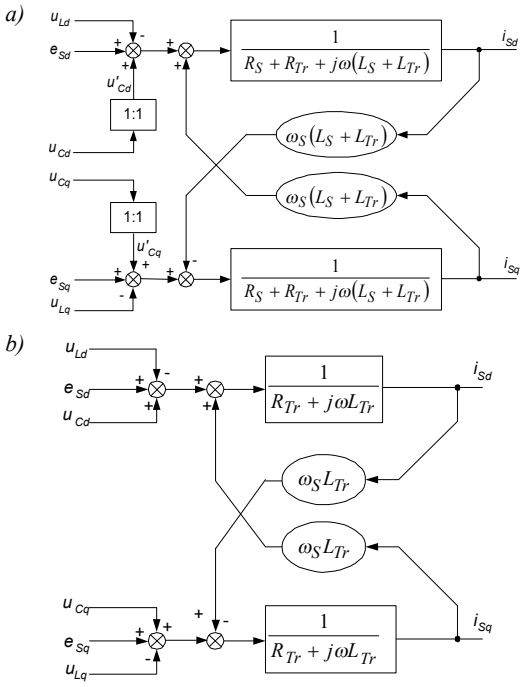

Fig.2. Block diagram of the supply line: a) considering network impedance; b) simplified.

3.2. Model of the SAPF with PWM controller

SAPF's major task is to compensate deformations in the network voltage, in this also higher harmonic. Therefore it is required high dynamics and exactness in voltage u_C formation. In case of utilization of the output filter L_V–C_V this is possible to realize this with help of the: 1) state-spaces regulator [29]; 2) voltage regulator with internal coupling in regard of capacitor's C_V current [16]. In elaborated model presented in Fig.4 there was assumed second regulator, complying temporary tendencies in changes of the output voltage ($C_V \cdot du_C/dt$).

Scheme presented in Fig.4 shows also the manner for realization of the state-spaces' double "decoupling". In "decoupling" circuit there are used measured temporary values of the capacitor's current as well as choke's in filter L_V-C_V current. This is no need to exact identify the capacitor capacity. In case, when state-spaces regulator is applied, this is match more easy to measure filter's output current to get the double "decoupling".

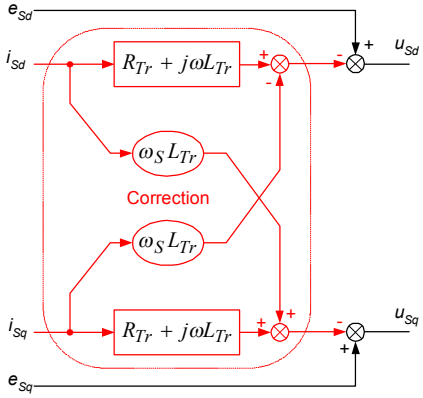

Fig.3. Block diagram of the arrangement for supply voltage measurement without and with correction of the transformer's influence.

3.3. Model of the PAPF with PWM controller

In PAPF, the questions of compensating current i_C formation are quite the same as questions of voltage u_C formation in SAPF. Also in PAPF there are applied the output filters L_I –C_I. Such filters are required in regard of disturbances and consequences of uncompensated outgrowths di_L/dt. If such filters are installed, it is advisable, for regulator to realize also the double "decoupling" of the state-spaces. Manner of double "decoupling" in PAPF, is analogous to described in previous section, as it is in Fig.5. Introduced there block diagram of the PAPF's differs from diagram of the SAPF's (Fig.4) because of lack of circuit for voltage on capacitance C_I control (load voltage u_L).

Fig.4. Block diagram of the SAPF with PWM controller and output filter.

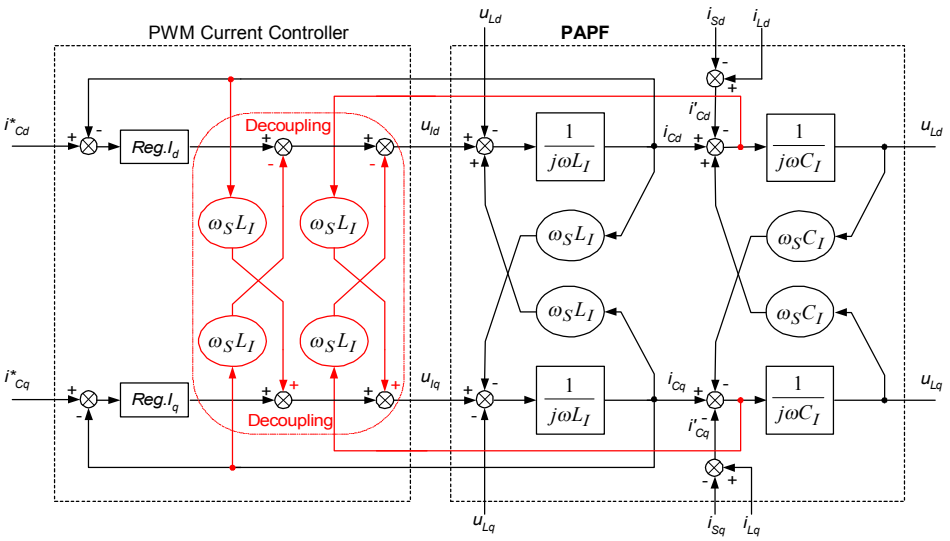

Fig.5. Block diagram of the PAPF with PWM controller and output filter.

3.4. Model of the DC circuit

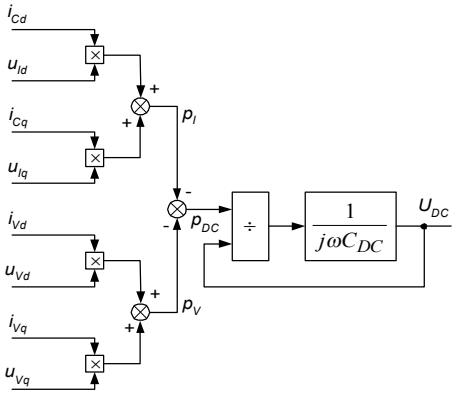

Fig.6. Block diagram of the DC circuit.

Presented in Fig.6, block diagram of the DC circuit, results from balance of instantaneous powers. Each deviation from zero in sum of the instantaneous active powers p_V and p_I, causes changes of the instantaneous U_{DC} voltage, in accordance with dependency:

$$C_{DC} \cdot U_{DC} \frac{dU_{DC}}{dt} = p_{DC} = -(p_V + p_I) = p_S - p_V \quad (2)$$

From dependency (2) as well as equation (1) results in obvious way, that sum of the instantaneous powers $p_V + p_I$ in steady state has to change periodically.

Model (Fig.6) omits power losses in SAPF and PAPF arrangements, profitably slowing U_{DC} voltage changes. Accepting such simplification, it is also possible to skip losses in LC filters as well as in transformer. In this case instantaneous power in DC link can be expressed by the following dependency:

$$p_V + p_I = \underbrace{i_{Sd}u_{Cd} + i_{Sq}u_{Cq}}_{p_V} + \underbrace{i_{Cd}u_{Ld} + i_{Cq}u_{Lq}}_{p_I} \quad (3)$$

3.5. Model of the load

In Fig.7, block diagrams of the loads were introduced. Voltage model (Fig.7a) in peculiarity should be used in case when UPQC is burden with diode rectifier with capacitive filter or in situation of UPQC usage to power flow control between two network supply sources. From the other side current model (Fig.7b) should be used, when as load e.g. thyristor rectifier with smoothing choke is used. Such rectifier, is often considerated as standard non-linear load, it also made up the test burden for UPQC arrangement (Fig.1), studied in this paper.

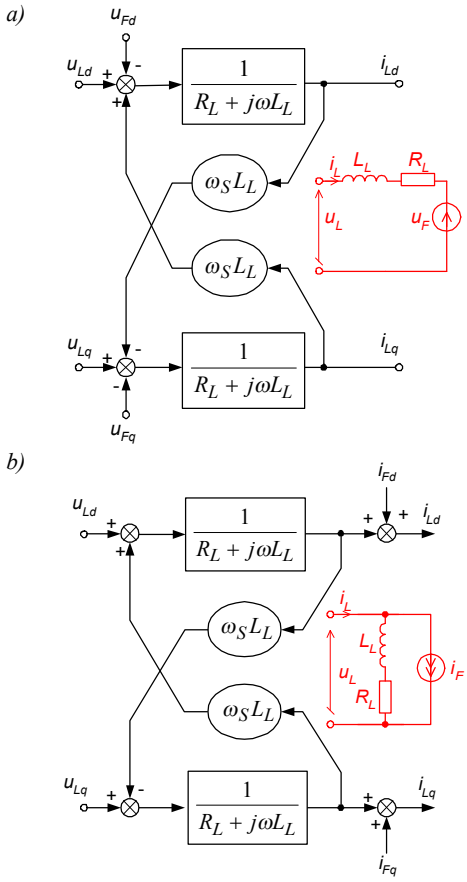

Fig.7. Block diagrams of the loads: a) voltage; b) current.

3.6. Model of the main controller

In UPQC's main controller, which model was introduced in Fig.8, adding voltage and current reference courses (u^*_C i i^*_C) are determined in two independent circuits. Input signals in first circuit (Fig.8a) there are given (set) courses of the load voltage u^*_L and measured source voltages u_S. First circuit does not take part in U_{DC} voltage stabilization as well as undesirable in load current i_L components compensation/filtration. This is the domain of the second circuit in main controller (Fig.8b).

To stabilize voltage U_{DC}, from compensating courses extracted in second circuit by the $F_L(j\omega)$ filters, there are subtracted the reference active components i^*_{Dd} and i^*_{Dq} of the PAPF's output current. Those components, determined on the basis of instantaneous power theory on the base of the following dependencies [8, 16]:

$$i^*_{Cd} = \Delta p^*_{DC} \frac{u_{Ld}}{u^2_{Ld} + u^2_{Lq}}, \quad i^*_{Cq} = \Delta p^*_{DC} \frac{u_{Lq}}{u^2_{Ld} + u^2_{Lq}} \qquad (4)$$

where: Δp^*_{DC} - exit signal in the voltage regulator, they cause faster or slower charging/discharging of C_{DC} capacitance, in dependency on value and sign of an error signal $\Delta U_{DC}=U^*_{DC}-U_{DC}$.

a)

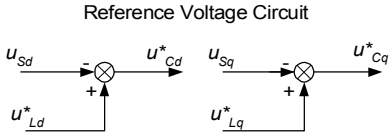

b)

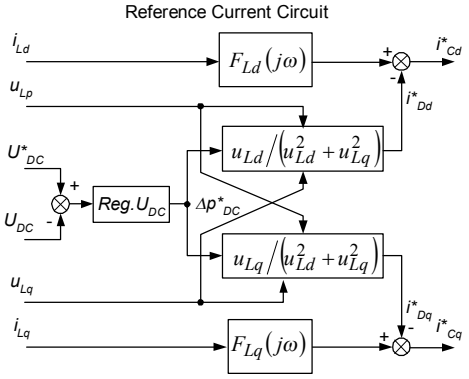

Fig.8. UPQC's main controller - block diagram.

3.7. Model of the complete UPQC

Elaborated full model contains models of the individual circuits described in 3.1÷3.6 as well as all connections between them. Model concerns the UPQC arrangement simultaneously fulfilling the following functions: harmonics compensation as well as network voltage stabilization and symmetrization, and also compensator of the passive components in load current. In this case, and when rotating „*d-q*" coordinates are suitably synchronized with the network voltage, the main controller become a very simple arrangement (Fig.9), obligatory containing only one High Pass Filter (e.g. differential module with T_R reference in limits 10-20 ms), suitable adders as well as voltage U_{DC} regulator - usually PI or inert P. Such simple main controller was also considered in UPQC's full block diagram, introduced in Fig.10.

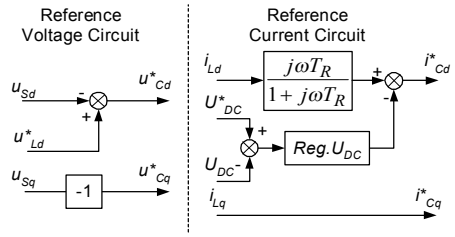

Fig.9. UPQC's simple main controller - block diagram.

UPQC's complete model (Fig.10) was elaborated with destination to investigate its filtration-compensation proprieties in often met in practice conditions of small network impedance (Fig.2b) and large internal impedance of the non-linear current load (Fig.7b). On the base of above, in this model, supply line parameters R_S and L_S as well as current load parameters R_L and L_L were skipped. Additionally, all regulators in SAPF's and PAPF's PWM controllers were accepted as P type. In this model in obvious way can also be implemented different types of regulators. However one should mark, that P type regulators permit to shape enough exactly the non-sinusoidal adding voltages and currents (u_C and i_C) [16] and do not inject additional dynamic errors during following the standard compensating courses.

Investigations of the dynamic processes in full model of the UPQC's arrangement (Fig.10) have confirmed presumption about small influence of the fast dynamic processes, connected with formation of the standard courses, onto considerably slower processes occurring both in DC circuit as well as connected with the standard courses determination. In case of investigations fast dynamic processes, SAPF and PAPF arrangements can be considered independently. To investigate the slow dynamic processes, usually good enough is simplified model. Such model was introduced in Fig.11. This model differs from the full one (Fig.10) because of replacement of the individual models of the SAPF and PAPF and their controllers onto ideal voltages and compensating currents adding sources. Carried out, onto this basis, the simple analysis of processes of charging/discharging the C_{DC} capacitance in DC circuit, is an object of the next chapter.

4. ANALYSIS OF THE PROCESSES IN DC CIRCUIT

To simplify the following analysis, one should initially notice, that the main controller from principle of operation can exclude the appearance of the some current and voltage components in UPQC arrangement. In case of controller from Fig.9, we always have e.g.:

$$\tilde{i}_{Sd} = 0\,,\ \tilde{i}_{Sq} = 0\,,\ \bar{i}_{Sq} = 0\,,\ \tilde{u}_{Ld} = 0\,,\ \tilde{u}_{Lq} = 0\,,\ \bar{u}_{Lq} = 0\,,$$
$$\bar{u}_{Sq} = 0$$

where: signs $\bar{u}, \bar{i}$ concerns the permanent components, and $\tilde{u}, \tilde{i}$ the pulsation components in currents and voltages.

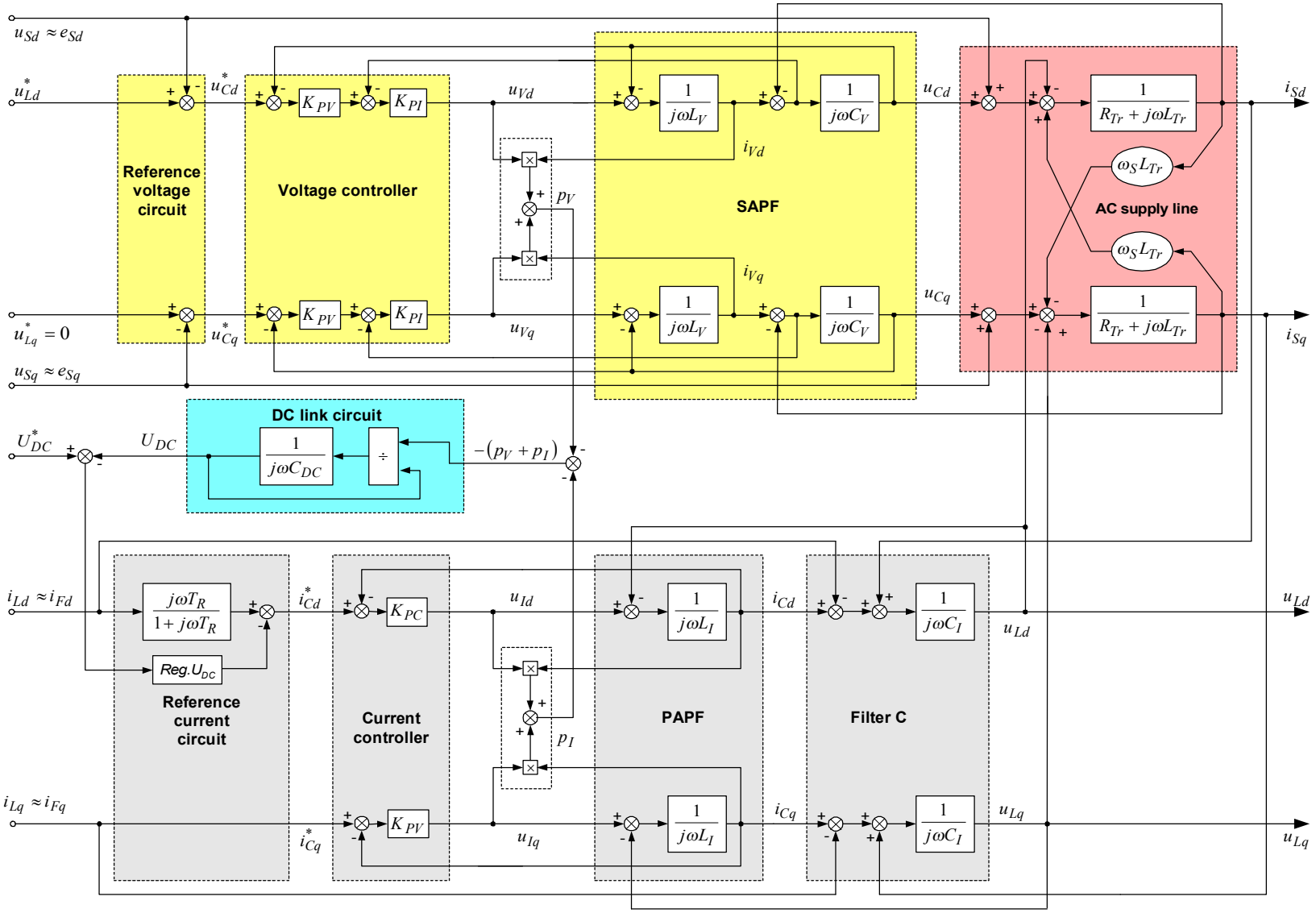

Fig.10. Block diagram of the complete UPQC with omission of the influence of supply network impedance.

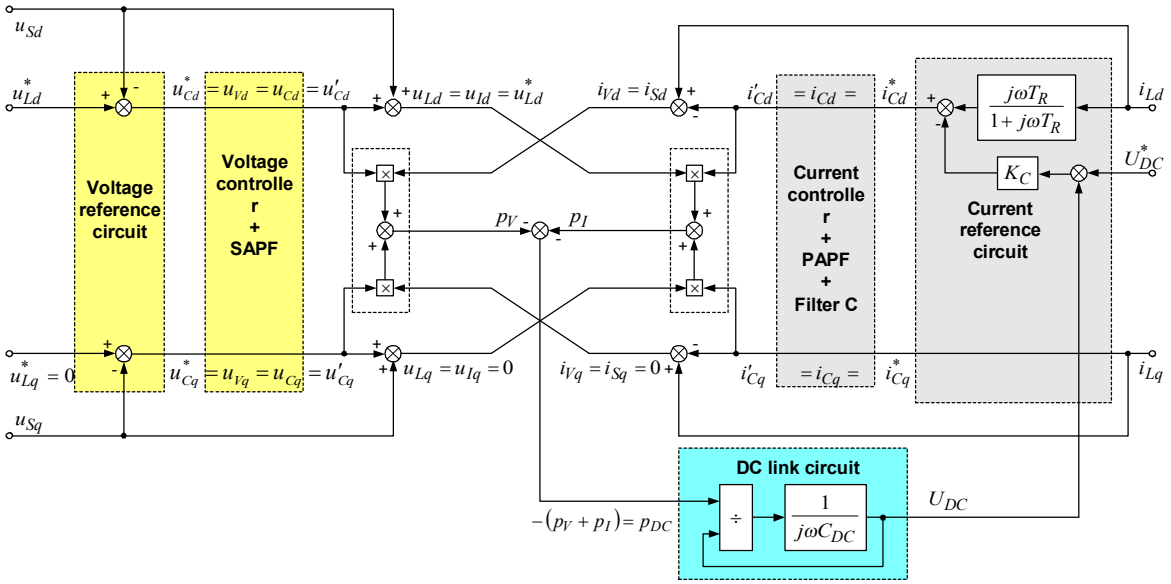

Fig.11.Simplified, with ideal voltage and current adding sources, model of the UPQC.

Taking into consideration above, and in accordance with accepted symbols, instantaneous power p_{DC} delivered to the DC link can be determined on the basis of the following dependency:

$$p_{DC} = \underbrace{\bar{i}_{Sd}\left(\bar{u}_{Sd}+\tilde{u}_{Sd}-\bar{u}_{Ld}\right)}_{-p_V}+\underbrace{\bar{u}_{Ld}\left(\bar{i}_{Sd}-\bar{i}_{Ld}-\tilde{i}_{Ld}\right)}_{-p_I}= \\ =\underbrace{\left(\bar{i}_{Sd}\bar{u}_{Sd}-\bar{u}_{Ld}\bar{i}_{Ld}\right)}_{\Delta P_{=}}+\underbrace{\left(\tilde{i}_{Sd}\tilde{u}_{Sd}-\tilde{i}_{Ld}\bar{u}_{Ld}\right)}_{\Delta P_{\sim}} \tag{5}$$

The partition of the instantaneous active power p_{DC} on two components $\Delta P_{=}$ as well as $\Delta P_{\sim}$ is connected with their different influences onto U_{DC} voltage changes during steady states as well as during transients.

4.1. Steady state

During steady state the component $\Delta P_{=}$=0, and the pulsation frequencies in periodic component $\Delta P_{\sim}$ depends only on harmonics, network voltage asymmetry and load current.

Lets consider that $\Delta P_{\sim}$ component is a superposition of the two sinusoidal courses with frequencies $\tilde{\omega}_U$ and $\tilde{\omega}_I$

$$\Delta P_{\sim} \approx P_L\left[K_{SU}\,sin\left(\tilde{\omega}_U t\right)-K_{LI}\,sin\left(\tilde{\omega}_I t+\varphi_{L/S}\right)\right] \tag{6}$$

where: $\varphi_{L/S}$ – phase shift between courses; K_{SU}, K_{SI} – coefficients determining influence of the every one of the sinusoidal courses on $\Delta P_{\sim}$ component; P_L – average active power of the load.

In this case and on the base of the following dependencies (2),(5) and (6) we do have:

$$\frac{C_{DC}}{2}\left[U^2_{DC(\max)}-U^2_{DC(\min)}\right]= \\ =2P_L\sqrt{\left(\frac{K_{SU}}{\tilde{\omega}_U}\right)^2-2\frac{K_{SU}K_{LI}}{\tilde{\omega}_U\tilde{\omega}_I}\sin\varphi_{L/S}+\left(\frac{K_{LI}}{\tilde{\omega}_I}\right)^2} \tag{7}$$

where: $U_{DC(\min)}$ – minimum, $U_{DC(\max)}$ - maximum voltage value on the C_{DC} capacitance.

From dependency (7) results, that the biggest U_{DC} pulsations ($U_{DC(\max)}$-$U_{DC(\min)}\rightarrow$ max) occur for $\varphi_{L/S}=3\pi/2$. From dependency (7) outcomes also the following equation:

$$\frac{C_{DC}}{2}\left(U_{DC(max)}-U_{DC(min)}\right)\left(U_{DC(max)}+U_{DC(min)}\right)\le \\ \le 2P_L\left(\frac{K_{SU}}{\tilde{\omega}_U}+\frac{K_{LI}}{\tilde{\omega}_I}\right) \tag{8}$$

Taking into consideration that:

$$U^*_{DC}=\left(U_{DC(\max)}+U_{DC(\min)}\right)/2\,,$$

and that the maximum error of the U_{DC} voltage is:

$$\Delta_{U(\max)}=U_{DC(\max)}-U^*_{DC}=U^*_{DC}-U_{DC(\min)}= \\ =\left(U_{DC(\max)}-U_{DC(\min)}\right)/2\,,$$

after some algebraic transformations dependency (8) can be rewritten as:

$$C_{DC}\le\frac{P_L}{\Delta_{U(max)}U^*_{DC}}\left(\frac{K_{SU}}{\tilde{\omega}_U}+\frac{K_{LI}}{\tilde{\omega}_I}\right) \tag{9}$$

Equation (9) can be also used in the following form:

$$C_{DC}\le\frac{P_L}{\varepsilon_C U^{*2}_{DC}}\left(\frac{K_{SU}}{\tilde{\omega}_U}+\frac{K_{LI}}{\tilde{\omega}_I}\right) \tag{10}$$

where: $\varepsilon_C=\dfrac{\Delta_{U(max)}}{U^*_{DC}}=\dfrac{U_{DC(max)}-U_{DC(min)}}{U_{DC(max)}+U_{DC(min)}}$ - maximum relative error of the U_{DC} voltage.

Coefficients K_{SU}, K_{SI} from dependences (6)-(10) should be even with the deformation coefficients of u_{Sd} as well as i_{Ld} courses:

$$K_{SU}=U_{SD}/U_{SP}\,;\quad K_{LI}=I_{LD}/I_{LP} \tag{11}$$

where:

$$U^2_{SP}=\frac{1}{2\pi}\int_0^{2\pi}\left(\bar{u}_{Sd}(\vartheta)\right)^2 d\vartheta\quad U^2_{SD}=\frac{1}{2\pi}\int_0^{2\pi}\left(\tilde{u}_{Sd}(\vartheta)\right)^2 d\vartheta$$

$$I_{LP}^2 = \frac{1}{2\pi}\int_0^{2\pi}\left(\bar{i}_{Ld}\right)^2 d\upsilon \; ; \; I_{LD}^2 = \frac{1}{2\pi}\int_0^{2\pi}\left(\tilde{i}_{Ld}(\vartheta)\right)^2 d\vartheta \; .$$

Frequencies $\tilde{\omega}_U$ and $\tilde{\omega}_I$ are picked up as the lowest, among spectrum components $\tilde{u}_{Sd}$ and $\tilde{i}_{Ld}$.

Determined on the base of dependence (9) or (10) C_{DC} value is inflated in relation to the required for correct during steady stats UPQC operation. Exacter results give weighed coefficients, considering the full spectra of u_{Sd} and i_{Ld} courses, although in practice their determination is not intentional. Capacity C_{DC} is determined mostly by the transient states during load active power step changes and/or network voltage amplitude changes.

4.2. Transient states

Let's consider, that in UPQC, which model was introduced in Fig.11 occurred load active power step change ΔP_L (e.g. additional load is on). This change, at constant voltage

$$u_{Ld} = \bar{u}_{Ld} = const$$

and with omission higher harmonic, it is identified as load current increase

$$\Delta\bar{i}_{Ld} = \Delta P_L / u_{Ld} \tag{12}$$

From here, in case of application of the reference current circuit as it is in Fig.9, the compensating current i_{Cd} changes are following the course:

$$\Delta\bar{i}_{Cd} = \frac{\Delta P_L}{u_{Ld}} e^{-\frac{t}{T_R}} + K_C \cdot \Delta U_{DC} \tag{13}$$

where: K_C - gain of the U_{DC} regulator (type P).

Because $i_{Ld} = i_{Sd} + i_{Cd}$, therefore load (12) and compensating (19) current changes crate also the network current change:

$$\Delta\bar{i}_{Sd} = \frac{\Delta P_L}{u_{Ld}}\left(1 - e^{-\frac{t}{T_R}}\right) - K_C \cdot \Delta U_{DC} \, ,$$

Together with this change, considering (5), component $\Delta P_=$ of the instantaneous power p_{DC} is changed also:

$$\Delta P_= = u_{Sd}\left[\frac{\Delta P_L}{u_{Ld}}\left(1 - e^{-\frac{t}{T_R}}\right) - K_C \cdot \Delta U_{DC}\right] - \Delta P_L$$

One can present above equation as:

$$\Delta P_= = \Delta P_L \cdot (\mu_u - 1) - \mu_u \cdot \Delta P \cdot e^{-\frac{t}{T_R}} - K'_C \cdot \Delta U_{DC} \tag{14}$$

where: $\mu_u = u_{Sd} / u_{Ld}$; $K'_C = u_{Ld} \cdot \mu_u \cdot K_C$

On basis of equation on charging the DC link capacitance (2) (linearized in U_{DC}^* surroundings), considering (14) as well as assuming without loss of generality μ_u=1, we receive:

$$\frac{d\Delta U_{DC}}{dt} = -\frac{K'_C}{C_{DC}U_{DC}^*} \cdot \Delta U_{DC} - \frac{\Delta P_L}{C_{DC}U_{DC}^*} \cdot e^{-\frac{t}{T_R}} \tag{15}$$

Equation (15) has the following solution:

$$\Delta U_{DC} = -\frac{\Delta P_L}{K'_C} \cdot \frac{T_R}{(T_R - T_C)} \cdot \left(e^{-\frac{t}{T_R}} - e^{-\frac{t}{T_C}}\right) \tag{16}$$

where:

$$T_C = C_{DC}U_{DC}^* / K'_C \tag{17}$$

On the base of dependency (16), changes of the voltage $\Delta U_{DC} = U_{DC} - U_{DC}^*$ are with one extremum, taking place after time t_{sup}, counted from the moment of occurrence of the load power ΔP_L step change:

$$\frac{d\Delta U_{DC}}{dt} = 0 \Leftrightarrow \frac{T_C T_R}{T_R - T_C} \ln\frac{T_R}{T_C} = t_{sup}$$

After putting value t_{sup} to dependency (16) and transformations we do have:

$$\Delta U_{DC(max)} = -\frac{\Delta P_L}{K'_C} \cdot \left(\frac{T_C}{T_R}\right)^{\frac{T_C}{T_R - TC}} \tag{18}$$

Value $\Delta U_{CD(max)}$ this is the maximum deviation of voltage U_{DC} from the reference value U_{DC}^*. This is easy to exert that:

$$\left|\Delta U_{DC(max)}\right| < \frac{\left|\Delta P_L\right|}{K'_C} \cdot \left(\frac{T_R}{T_C + T_R}\right)$$

Considering (17), we do have:

$$\left|\Delta U_{DC(max)}\right| < \frac{\left|\Delta P_L\right| \cdot T_R}{C_{DC} \cdot U_{DC}^* + K'_C \cdot T_R} \tag{19}$$

Dependency (19) allows in practical and simple way to evaluate influence: main controller's T_R and K_C coefficients, reference value U_{DC}^*, C_{DC} capacitance and load power ΔP_L step changes on maximum deviation $\Delta U_{CD(\max)}$. Values $\Delta U_{DC(\max)}$ as a function of increases ΔP_L calculated on the base of (19) and received experimentally were compared in chapter 5.

C_{DC} capacitance, determined on the base of equation:

$$C_{DC} = \frac{T_R}{U_{DC}^*} \cdot \frac{\left|\Delta P\right| - K'_C \cdot \left|\Delta U_{DC(\max)}\right|}{\left|\Delta U_{DC(\max)}\right|} \cdot \tag{20}$$

it guarantees, that voltage U_{DC} do not exceed the admissible range of changes. Theoretically possible negative C_{DC} value is result of linearization of equation (2). In practice such negative value is impossible, because of required small deviations of $\Delta U_{DC(max)}$ as well as limited value of K_C', determined with regard of sensor ratio. Too large value of K_C' can be connected with stability problems.

Summing up this chapter one should note, that C_{DC} capacity in UPQC should be selected with regard of the worst cases, as the largest value from two calculated on the base of equations (9) as well as (20):

$$C_{DC} = max\left[C_{DC}(9), C_{DC}(20)\right] \tag{21}$$

Only then the condition about un-exceeding the admissible $\Delta U_{DC(\max)}$ changes, during steady states as well as during transient will be secured.

5. EXPERIMENTAL RESULTS

In Fig.12 one can see the laboratory stand to investigate the small power experimental model of the UPQC (Fig.1). In arrangement the simple main controller was applied (Fig.9) with P type regulator for U_{DC} voltage control. Selected parameters and adjustables of the laboratory model are introduced in Table 1. Further presented results of investigations contain steady states and transients as well as UPQC capabilities to power flow control between two voltage sources.

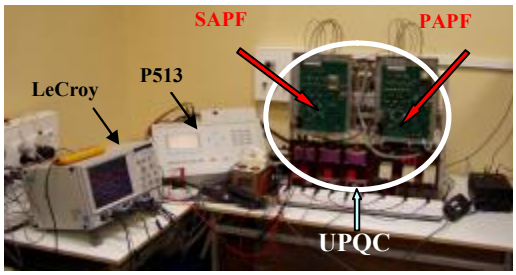

Fig.12. Experimental model for investigations of UPQC.

Tab.1. Selected parameters and adjustables of the UPQC.

Nominal network voltage U_S	*3×220 V*
Admissible range of changes in network voltage	*60÷340 V*
Stabilized load voltage U_L	*3×60÷240 V*
DC link capacitor	*1650 μF*
The reference voltage U^*_{DC} in DC	*610 V*
The maximum network current $I_{S(max)}$	*20 A*
In the main controller, HPF time constant T_R	*10 ms*
K_C gain in the U_{DC} voltage regulator (with assumption of the sensor 0,052 V/V)	*1 V/V*
PWM frequency in PAPF controller	*4 kHz*
PWM frequency in SAPF controller	*12 kHz*

5.1. Results obtained during steady states

In Fig.13 the exemplary simulation and experimental current and voltage courses, illustrating UPQC's filtration capabilities in steady states, were introduced. Experimental courses concern situation when arrangement is burdened with controlled 6-pulse rectifier (α=0º, $THD(I_L)$≈28%) with power 7 kW and supplied with deformed network voltage with distortion coefficient $THD(U_S)$≈9%. Both current i_S as voltage u_L in this of case are practically sinusoidal.

UPQC filtration proprieties only in slight degree depend on load power (Fig.14). Increase of $THD(I_S)$ coefficient at small load is related to enlarged participation of harmonics with frequency of the PWM sawtooth carrier in PAPF controller. Increase of $THD(U_L)$ coefficient at enlarged load is related to voltage drop on adding transformer's impedance, caused by the uncompensated load current harmonics. One should mark, that such changes of $THD(U_L)$ and $THD(I_S)$ show the improperly selected passive filters *L-C* in UPQC arrangement (Fig.1).

Load changes mainly infect the PAPF and SAPF nominal powers (Fig.15). In general case, nominal power of the PAPF's depends on distortion power, reac-

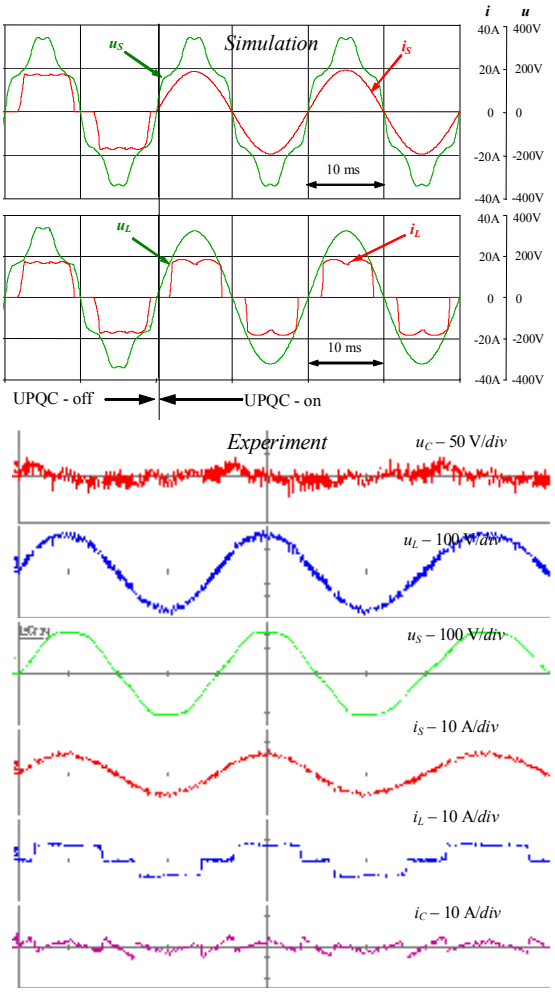

Fig.13. Simulation and experimental courses in case of the network voltage and load current harmonics compensation.

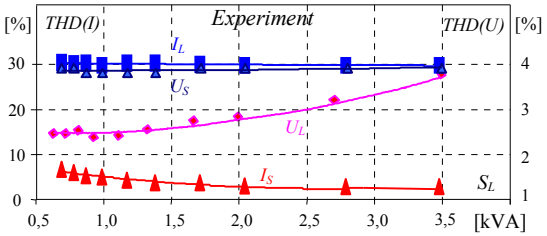

Fig.14. Current and voltage THD coefficients as a function of the apparent power of load (α=0º).

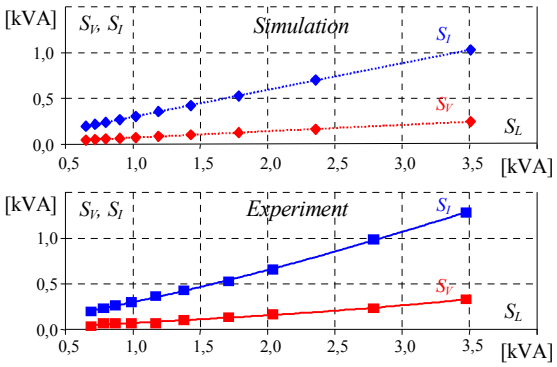

Fig.15. SAPF (S_V) and PAPF (S_I) nominal power as a function of the apparent power of the load (α=0º).

tive and unsymmetrical power of the load, additionally nominal power of the SAPF's depends on active component in load current as well as value, deformations and asymmetry of the network voltage. Simulation and experimental dependencies, introduced in Fig.15, concern only case when UPQC is supplied with sinusoidal ($THD(U_S)$≈4%) and symmetrical nominal voltage, and burdened with 6-pulse rectifier.

The nominal powers depends also, however in smaller degree, on SAPF and PAPF efficiency. Increasing load power (and network voltage) participation of losses in nominal power components decreases. The same dependency concerns also in obvious way the efficiency of the whole UPQC arrangement (Fig.17). In boundary studied case S_L= 8,5 kVA (not in Fig.17) measured efficiency of laboratory model carried out 0,96.

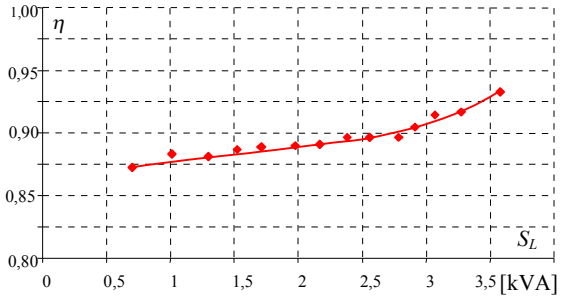

Fig.16. UPQC efficiency as a function of the apparent power of the load (α=0°).

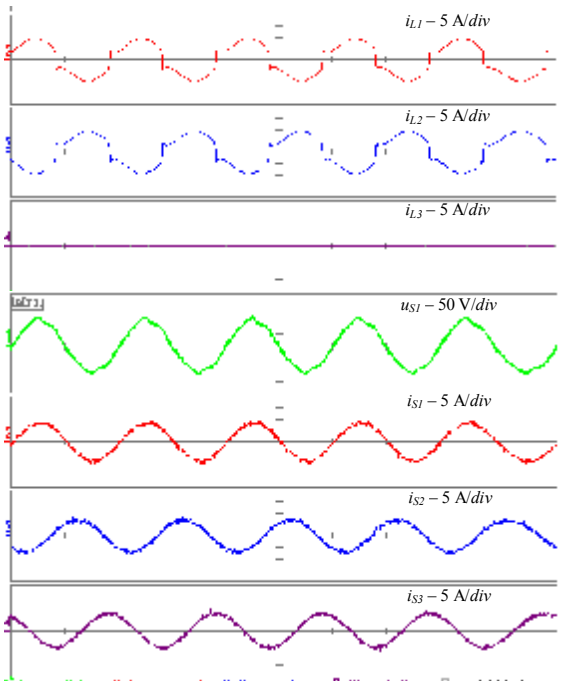

Fig.17. Experimental courses in case of symmetrical supply and non-linear and non-symmetrical load.

Experimental investigation of the UPQC arrangement in steady states contained also estimation of possibility of realization through this arrangement function of the load as well as network voltage symmetrization. Investigations were realized at lowered supply (network) voltage. Two, 2-pulse rectifiers 1,1 kVA apparent power each, made up the asymmetrical load. Amplitude asymmetric supply (network) voltage was obtained with assistance of three independent autotransformers. Exemplary results of experiment illustrate, introduced in Fig.17 and Fig.18, current and voltage courses.

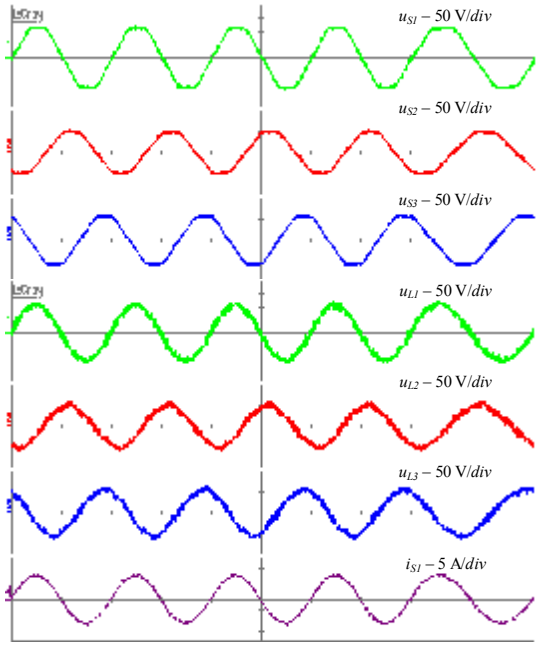

Fig.18. Experimental courses in case of non-symmetrical supply and symmetrical resistive load.

5.2. Results obtained during transients

Experimental verification of dependency (20) was the principle aim of this investigations. In theoretical calculations it was considered: adjustments T_R=10 ms and K_C=1V/V (Table 1), nominal value U_S=220 V i.e. u_{Sd}=400 V (look Appendix), the reference value U^*_{DC} =610 V, as well as gain μ_u= 0,052 of the voltage U_{DC} sensor in real laboratory model. Allowing at this deviation $\Delta U_{DC(max)}$=30 V and load active power step (Δt=0) changes $\Delta P_L < \Delta P_{L(max)}$=4 kW, calculated C_{DC} value carried out 1850 μF. In laboratory model, from practical point of view, capacitor with smaller capacity C_{DC} =1650 μF, was applied. This capacity concern also dependences introduced in Fig.18.

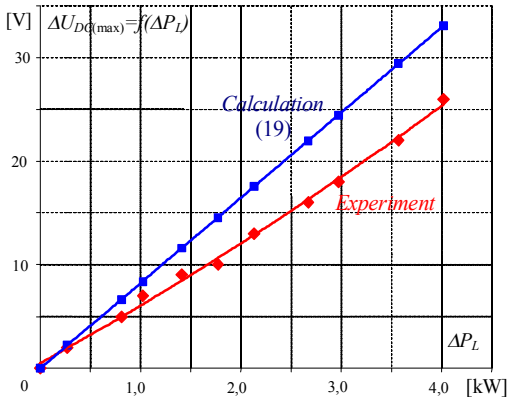

Fig.19. Maximum deviations of the U_{DC} voltage from the reference value U_{DC}^* ($\Delta U_{DC(max)}=U_{DC(max)}-U_{DC}^*$) as a function of increases ΔP_L.

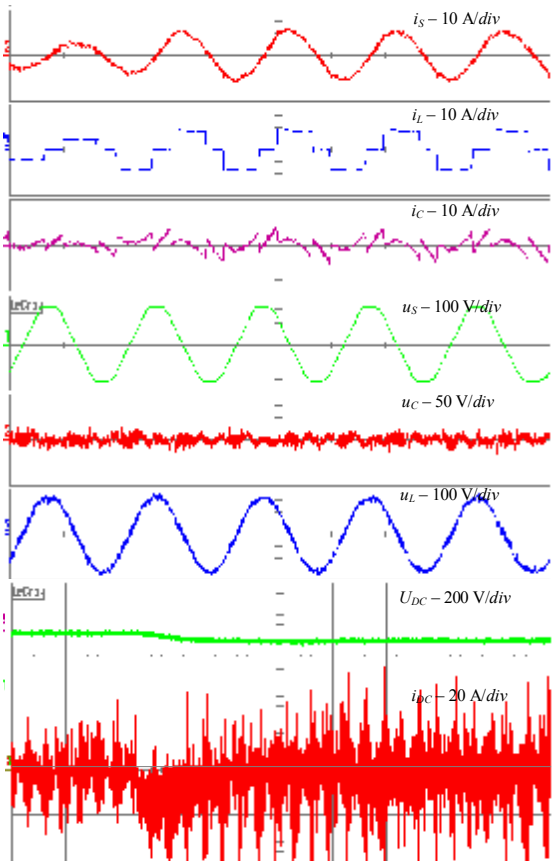

Fig.20. Experimental courses in case of harmonics filtration and load step changes ΔP_L from 4kW to 8kW.

5.3. Additional functions – power flow control

UPQC arrangement with success can be used to power flow control. Considering problem cognitively, power flow controller generally is a synchronous voltage source (SVS), presented as source of the adding u_C voltage with frequency dependent on network frequency with possibility of control of its voltage amplitude in range $0 \le U_C \le U_{Cmax}$ and angle γ in limits: $0 \le \gamma \le 2\pi$, connected with transmission line as this in Fig.21. In UPQC arrangement, SAPF exchanges with transmission line both active power (series active compensation) as passive power (series reactive compensation), thanks what there is possible to power flow control. However active power exchange, which affects mostly reactive power, is connected with consumption from DC circuit the active power. Therefore the main purpose of the PAPF's is U_{DC} voltage stabilization.

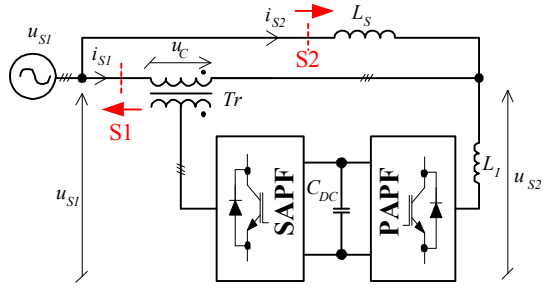

Fig.21. Connection scheme to investigate UPQC's capabilities for power flow control.

UPQC, behaving as power flow controller, can be controlled in accordance with rules presented in Fig.22. The vector diagram from Fig.22a. introduces situation, when adding voltage has constant amplitude U_C=const, in this case only angle γ is changed in range $(0 \div 2\pi)$. Such way of control cases however, variable voltage load U_{S2}. If voltage U_{S2} has to be stabilized, UPQC should be controlled in accordance with rule introduced in Fig.22b. In this case there are changed: amplitude of adding voltage U_C as well as angle δ.

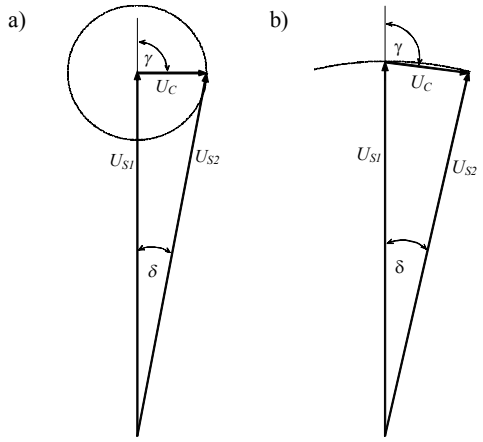

Fig.22. Vector diagrams for the arrangement presented in Fig.21, in case when power flow control is achieved through: a) changes of the γ angle, maintaining constant u_C voltage, b)changes of the δ angle, maintaining even voltages u_{S1} and u_{S2}.

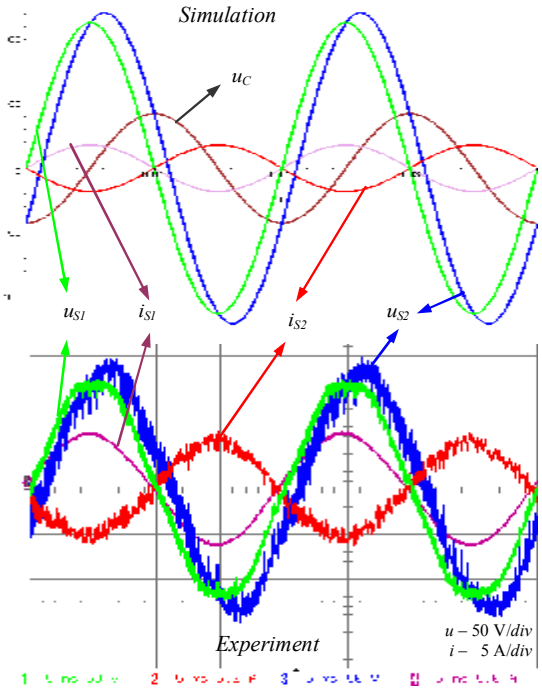

Fig.23.Example simulation and experimental courses obtained in arrangement presented in Fig.21 in case when power flow control is on the base of rule explained in Fig.22a.

In Fig.23 simulation and experimental voltage and current courses, for UPQC arrangement working in accordance with rule from Fig.22a, were introduced. As one can see experimental and simulation results agree, however such control causes changes in load voltage

U_{S2}. Characteristics of changes of active and reactive power as a function of variable angle γ are presented in Fig.24. As one can see, characteristics confirm the UPQC's power flow control capabilities.

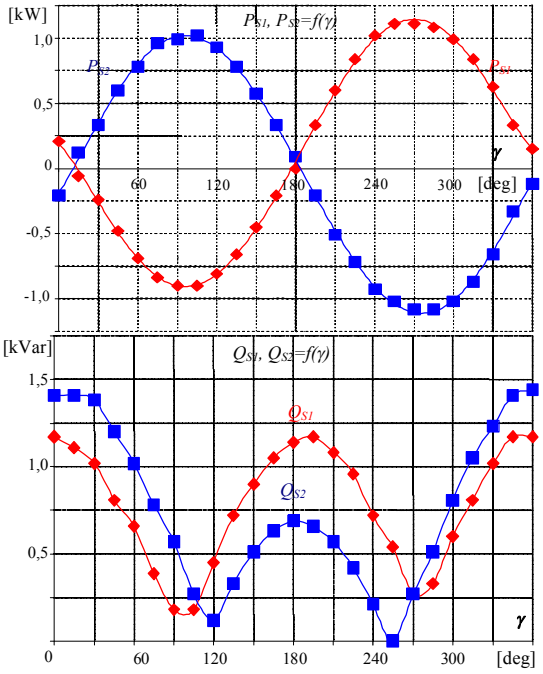

Fig.24. Active and reactive powers, measured at S1 and S2 points of the arrangement from Fig.21, as a function of γ angle. Constant u_C voltage.

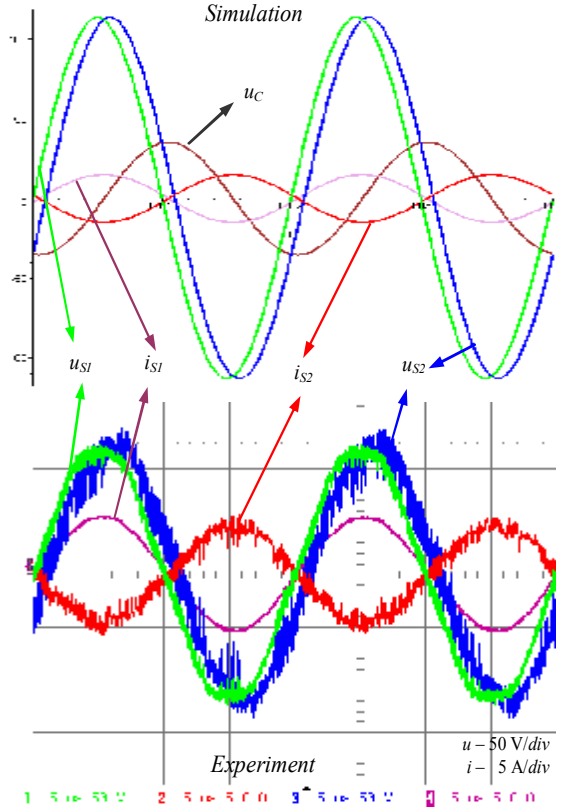

Fig.25. Example simulation and experimental courses obtained in arrangement presented in Fig.21 in case when power flow control is on the base of rule explained in Fig.22b.

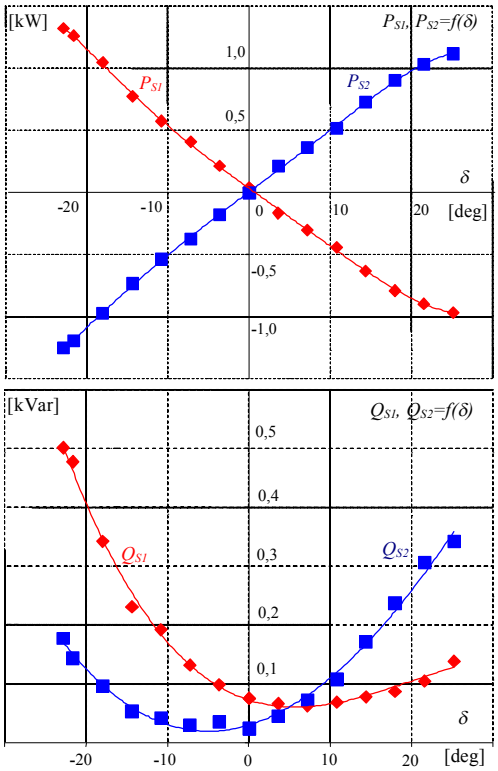

Fig.26. Active and reactive powers, measured at S1 and S2 points of the arrangement from Fig.21, as a function of δ angle. Even voltages u_{S1} and u_{S2}.

In Fig.25 simulation and experimental voltage and current courses, for UPQC arrangement working in accordance with rule from Fig.22b, were introduced. As one can see experimental and simulation results agree. Characteristics of changes of active and reactive power as a function of variable angle δ are presented in Fig.26. The second manner of control is equivalent to situation when SAPF exchanges with the transmission line mainly the reactive power (series reactive compensation). As a consequence predominantly in transmission line there is changed the active power, range of reactive power control is smaller than in first case (Fig.22a).

6. CONCLUSIONS

In this paper the basis of analytical modeling of the Unified Power Quality Conditioner arrangements in *d-q* rotating coordinates, as well as selected results of investigations conducted on the simplified small power laboratory model were talked over.

Created with minimum number of simplifying assumptions, UPQC full model (in *d-q* rotating coordinates) permits to entirely independent control in relation to *p* and *q* coordinates and particularly is useful in stability investigations and regulators' parameters as well as values of the passive elements selection. On this basis method for analytic determination of the DC link capacitance, coupling both parallel and series arrangements, was worked out and verified experimentally.

Simulation investigations, completed with experimental results, including among others operation of the UPQC arrangement in case of burden of the supply with

thyristor rectifier were next introduced. Results of both analyses (theoretical and experimental) are confirming good filtration-compensating proprieties as well as multi-functionality of the UPQC arrangements. Investigated UPQC arrangement simultaneously permits to fulfill the following functions: voltage and current harmonics compensation, network voltage and load current symmetrization as well as network voltage stabilization and power flow control.

7. REFERENCES

1. Gyugyi L., Strycula E.C.: *Active AC Power Filter*. IEEE/IAS Annual Meet. Conf. Rec., 1976, pp.529-535.
2. Malesani L., Rosseto L., Tenti P.: *Active filter for reactive power and harmonic compensation*. Conf. Rec. 17th Annual Meet. IEEE Power Electronic Council, 1986, 321-330.
3. Peng F.-Z., Akagi H., Nabae A.: A study of active power filters using quad-series voltage-source PWM converters for harmonic compensation. IEEE Tran. on Ind. Appl.. Vol.22, No.3, 1986, pp.460-465.
4. Peng F.Z., Akagi H., Nabae A.: *A Combined System of Shunt Active and Series Active Power Filters*," Transactions of the Inst. of Electrical Eng. of Japan) , Vol.109-D, No.12, 1989, pp.897 – 904.
5. Peng F.Z, et al: *Compensation characteristics of the combined system of shunt passive and series active filters*. IEEE/IAS Annual Meet. Conf. Rec., 1989, pp.956-966.
6. Fujita H., Akagi H.: A practical approach to harmonic compensation in power systems - series connection of passive and active filters. IEEE/IAS Annual Meet. Conf. Rec., 1990, pp.1107-1112.
7. Gyugyi L.: Unified Power Flow Control Concept for Flexible AC *Transmission Systems*. IEE Proc., Vol. 139, pt. C, No. 3, 1992, pp. 323-331.
8. Akagi H.: *Generalised theory of instantaneous reactive power in three-phase circuits*. Conf. Rec. IPEC'83, 1993, pp. 1375-1386.
9. Kowalski M., Strzelecki R.: *The hybrid filter of network current harmonics with the compoensation of the reactive component*. Proc. of the Conf. PEMC'94, 1994, pp.219-224.
10. Akagi H.: *New trends in active filters*. Conf. Proc. EPE'95, 1995, s. 0.017-0.026.
11. Moran L. et al.: *Line conditioning system with simple strategy and fast dynamic response*, IEE Proc.-Gener. Transm. Distribution, Vol. 142, No.2,, 1995, pp.128-.134
12. Peng, F.Z., Lai, J.S.: *Application Considerations and Compensation Characteristics of Shunt Active and Series Active Filters in Power Systems*. Proc. of the 7th Int. Conf. on Harmonics and Quality Power, 1996,p.12-20.
13. Aredes M., Heumann K.: *A unified power flow controller with active filtering capabilities*. Proc. of the Conf. PEMC'96, pp.3/139-3/144
14. Jeon S.-J., Cho G.-H.: A Series-Parallel Compensated Uninterruptible Power Supply with Sinusoidal Input Current and Sinusoidal Output Voltage. Proc of the Conf. PESC'97, 1997, pp.297-303
15. Morán L.A., Fernández L., Dixon J.W.: *A simple and low-cost control strategy for active power filters connected in cascade*. IEEE Trans. on Ind. Electronics, Vol.44, No.5, 1997 pp.402-408.
16. Strzelecki R., Supronowicz H.: *Harmonic filtration in AC Power Systems*. Adam Marszałek Publishing, Toruń, Wyd. 1/2, 1997/99. (in Polish)
17. Fujita H. and Akagi H., *Unified power quality conditioner: The integration of series and shunt active filter*. *IEEE Trans. Power Electron.*, Vol. 13, No. 2, 1998, pp. 315-322.
18. Aredes M., Heumann K., Watanabe E.H.: *An Universal Active Power Line Conditioner*. IEEE Trans. on Power Delivery,Vol.13, No.2, 1998, pp.1453-1460.
19. Strzelecki R., Benysek G., Frąckowiak L.: *Dynamic properties of hybrid filters in regenerative braking thyristor systems*. Proc of the Int. Conf. ISIE'96, 1996, pp.596-601.
20. Frąckowiak L., Strzelecki R.: *Hybrid filter operation during nonlinear current pulsation*. The Int. Jurnal "COMPEL", Vol.16, No.1, 1997, pp.38-48.
21. Strzelecki, R., Kukluk, J., Rusiski, J.: *Active power line conditioners based on symmetrical topologies*. Proc of the IEEE Int. Sym. ISIE'99 , Vl.2, 1999, pp. 825-830.
22. Fujita H., Watanabe Y., H. Akagi H.: *Control and analysis of a unified power flow controller*. IEEE Trans. Power Electronics, Vol.14, No.6, 1999, pp.1021-1027.
23. Strzelecki R., et al.: *A universal symmetrical topologies for active power line conditioners*, Proc. of the Conf. EPE '99 (CD-ROM), 1999, s.10.
24. El-Habrouk M., Darwish M.K., Mehta P.: *Active power filters: a review*. IEE Proceedings- Electric Power Applications. Vol.147, No.5, 2000, pp. 403-413.
25. Strzelecki R., Supronowicz H.: *Power factor in AC supply systems and improvements methods*, Publishing house of the Warsaw Univ. of Tech, 2000 . (in Polish)
26. Zhou L. and Smedley K.: *Unified Constant-frequency Integration Control of Single Phase Active Power Filter*, Proc of the IEEE Applied Power Electronics Conf., 2000.
27. Ghosh A., Ledwich G.: *A unified power quality conditioner (UPQC) for simultaneous voltage and current compensation*. Electric Power Systems Research, Vol. 59, 2001, pp. 55-63.
28. Elnady, A., Goauda A., Salama M.M.A.: *Unified power quality conditioner with a novel control algorithm based on wavelet transform*. Proc on the Canadian Conf. on Electrical and Computer Eng. Vol. 2, 2001, pp. 1041 – 1045.
29. Kaźmierkowski M.P., Krishnan R., Blaabjerg F.: *Control in Power Converters. Selected Problems*. Academic Press, 2002.

30. Malabika Basu M., Das S.P., Dubey G.K.: *Performance Study of UPQC-Q for Load Compensation and Voltage Sag Mitigation*. Proc. of the Conf. IECON'2002, 2002, pp. 698-702.
31. Ghosh A., Ledwich G., *Power Quality Enhancement using Custom Power Devices*, Kluwer Academic Publishers, Boston (2002)
32. Meckien G., Strzelecki R.: *Single Phase Active Power Line Conditioners - without Transformers*. Proc. of the Conf. EPE–PEMC'2002, 2002, CD-ROM, p.8.
33. da Silva, S.A.O., et al.: *A three-phase line-interactive UPS system implementation with series-parallel active power-line conditioning capabilities*. IEEE Tran. on. Ind. Appl., Vol. 38, No.6, 2002, pp.1581-1590.
34. Watanabe E.H., Aredes, M.: *Power quality considerations on shunt/series current and voltage conditioners*. Proc. of the 10th Int. Conf. on Harmonics and Quality of Power, Vol.2, 2002, pp. 595 – 600
35. Mossoba J., Lehn P., *A controller architecture for high bandwidth active power filters*, *IEEE Trans. Power Electron.*, Vol.18, Jan. 2003.
36. Oliveira da Silva S.A., et al.: *Performance analysis of three-phase line-interactive UPS system with active power-line conditioning*. Proc of the 29th Annual IEEE Conf. IECON'03, Vol.1, 2003, pp353-360.
37. Pengcheng Zhu, et al.: *A novel control scheme in 2-phase unified power quality conditioner*. Proc. of the 29th IEEE Annual Conf. IECON'2003, Vol.2, 2003, pp.1617-1622.
38. Ghosh, A., Jindal A.K., Joshi, A.: *Inverter control using output feedback for power compensating devices*. Proc of the Conf. TENCON'2003,Vol.1, 2003, pp.48-52.
39. Strzelecki R.: *New concepts of the conditioning and power flow control in the AC distribution systems*. Proc. of the V Int. Conf. "Modern Feed Equipments in Electrical Power Systems" , 2003, pp.65-72
40. Jin T., Li L., Smedley K.: *A universal vector controller for three-phase PFC, APF, STATCOM, and grid-connected inverter*. Proc. of the 19th IEEE Conf. APEC'04. Vol. 1, 2004, pp. 594 – 600.
41. Karimi-Ghartemani M., et al.: *A signal processing system for extraction of harmonics and reactive current of single-phase systems*. IEEE Tran. on Power Delivery, Vol.19, No.3, 2004, pp.979–986.
42. Donghua Chen, Shaojun Xie: *Review of the control strategies applied to active power filters*. Proc.of the 2004 IEEE Int. Conf. on Electric Utility Deregulation, Restructuring and Power Technologies, 2004. (DRPT'2004). Vol.2, 2004, pp.666–670.
43. Emadi A., Nasiri A., Bekiarov S.B.: *Uninterruptible Power Supplies and Active Filters*. CRC Press, 2004.
44. D. Wojciechowski, Control of PWM rectifier with prediction of electromotive force," Ph.D. Thesis, Gdansk Univ. of Tech. 2005 (in Polish).

APPENDIX

A1. The stationary phase (1-2-3) and rectangular coordinates (α-β-0)

The transformation between coordinates (1-2-3)↔(α-β-0) are given by:

$$\begin{bmatrix} y_\alpha \\ y_\beta \\ y_0 \end{bmatrix} = \sqrt{\frac{2}{3}} \begin{bmatrix} 1 & -1/2 & -1/2 \\ 0 & \sqrt{3}/2 & -\sqrt{3}/2 \\ 1/3 & 1/3 & 1/3 \end{bmatrix} \cdot \begin{bmatrix} y_1 \\ y_2 \\ y_3 \end{bmatrix}$$

$$\updownarrow$$

$$\begin{bmatrix} y_1 \\ y_2 \\ y_3 \end{bmatrix} = \begin{bmatrix} 2/3 & 0 & 1 \\ -1/3 & \sqrt{3}/3 & 1 \\ -1/3 & -\sqrt{3}/3 & 1 \end{bmatrix} \cdot \begin{bmatrix} y_\alpha \\ y_\beta \\ y_0 \end{bmatrix}$$

If $y_1+ y_2+ y_3=0$ (always in 3-wire supply networks), then $y_0=0$ and:

$$\begin{bmatrix} y_\alpha \\ y_\beta \end{bmatrix} = \sqrt{\frac{2}{3}} \begin{bmatrix} 1 & -1/2 & -1/2 \\ 0 & \sqrt{3}/2 & -\sqrt{3}/2 \end{bmatrix} \cdot \begin{bmatrix} y_1 \\ y_2 \\ y_3 \end{bmatrix}$$

$$\updownarrow \qquad \text{(A1)}$$

$$\begin{bmatrix} y_1 \\ y_2 \\ y_3 \end{bmatrix} = \begin{bmatrix} 2/3 & 0 \\ -1/3 & \sqrt{3}/3 \\ -1/3 & -\sqrt{3}/3 \end{bmatrix} \cdot \begin{bmatrix} y_\alpha \\ y_\beta \end{bmatrix}$$

A2. The rectangular stationary (α-β) and rotating coordinates (p-q)

Transformation between (α-β)↔(d-q) coordinates, with assumption $y_0=0$, is on the base of dependency:

$$\begin{bmatrix} y_d \\ y_q \end{bmatrix} = \underbrace{\begin{bmatrix} \cos\omega_S t & \sin\omega_S t \\ -\sin\omega_S t & \cos\omega_S t \end{bmatrix}}_{\Theta^{-1}} \cdot \begin{bmatrix} y_\alpha \\ y_\beta \end{bmatrix}$$

$$\updownarrow \qquad \text{(A2)}$$

$$\begin{bmatrix} y_\alpha \\ y_\beta \end{bmatrix} = \underbrace{\begin{bmatrix} \cos\omega_S t & -\sin\omega_S t \\ \sin\omega_S t & \cos\omega_S t \end{bmatrix}}_{\Theta} \cdot \begin{bmatrix} y_d \\ y_q \end{bmatrix}$$

or generally

$$Y_{dq} = \Theta^{-1} Y_{\alpha\beta} \quad \leftrightarrow \quad Y_{\alpha\beta} = \Theta Y_{dq}$$

or

$$y_p + jy_q = \left(y_\alpha + jy_\beta\right) \cdot e^{-j\omega_S t}$$

$$\updownarrow$$

$$y_\alpha + jy_\beta = \left(y_d + jy_q\right) \cdot e^{j\omega_S t}$$

A3. State space equations in (α-β) and (d-q) coordinates

$$\frac{dX_{\alpha\beta}}{dt} = \mathbf{A}_\beta^\alpha X_{\alpha\beta} + \mathbf{B}_\beta^\alpha F_{\alpha\beta}$$

$$\updownarrow \qquad \text{(A3)}$$

$$\frac{dX_{dq}}{dt} = \mathbf{A}_q^d X_{dq} + \mathbf{B}_q^d F_{dq}$$

where:

$$\mathbf{A}_{\beta}^{\alpha}=\begin{bmatrix}A_{\alpha\alpha} & A_{\alpha\beta}\\ A_{\beta\alpha} & A_{\beta\beta}\end{bmatrix},\quad \mathbf{B}_{\beta}^{\alpha}=\begin{bmatrix}B_{\alpha\alpha} & B_{\alpha\beta}\\ B_{\beta\alpha} & B_{\beta\beta}\end{bmatrix},$$

$$\mathbf{A}_{q}^{d}=\begin{bmatrix}A_{dd} & A_{dq}\\ A_{dp} & A_{qq}\end{bmatrix},\quad \mathbf{B}_{q}^{d}=\begin{bmatrix}B_{dd} & B_{dq}\\ B_{qd} & B_{qq}\end{bmatrix},$$

$$X_{\alpha\beta}=\begin{bmatrix}X_{\alpha}\\ X_{\beta}\end{bmatrix},\ F_{\alpha\beta}=\begin{bmatrix}F_{\alpha}\\ F_{\beta}\end{bmatrix},\ X_{dq}=\begin{bmatrix}X_{d}\\ X_{q}\end{bmatrix},\ F_{dq}=\begin{bmatrix}F_{d}\\ F_{q}\end{bmatrix}$$

Considering form of the transformation Θ (A2), let's determine dependencies between **A** and **B** matrices for the replacement of coordinates (*α*-*β*)↔(*p*-*q*). For this purpose, on the base of (A2) and (A3) one can write:

$$\frac{dX_{\alpha\beta}}{dt}=\frac{d}{dt}\left(\Theta\cdot X_{dq}\right)=\mathbf{A}_{\beta}^{\alpha}\cdot\Theta\cdot X_{dq}+\mathbf{B}_{\beta}^{\alpha}\cdot\Theta\cdot F_{dq},$$

and after transformations we do have:

$$\frac{dX_{dq}}{dt}=\underbrace{\Theta^{-1}\left(\mathbf{A}_{\beta}^{\alpha}\cdot\Theta-\frac{d\Theta}{dt}\right)}_{\mathbf{A}_{q}^{d}}\cdot X_{dq}+\underbrace{\Theta^{-1}\mathbf{B}_{\beta}^{\alpha}\cdot\Theta}_{\mathbf{B}_{q}^{d}}\cdot F_{dq}$$

On the base of above one can write:

$$\begin{aligned}\mathbf{A}_{q}^{d}&=\Theta^{-1}\cdot\mathbf{A}_{\beta}^{\alpha}\cdot\Theta-\Theta^{-1}\cdot\frac{d\Theta}{dt}\\ &\updownarrow\\ \mathbf{A}_{\beta}^{\alpha}&=\Theta\cdot\mathbf{A}_{q}^{d}\cdot\Theta^{-1}+\frac{d\Theta}{dt}\Theta^{-1}\end{aligned}\qquad\text{(A4)}$$

and

$$\mathbf{B}_{q}^{d}=\Theta^{-1}\mathbf{B}_{\beta}^{\alpha}\cdot\Theta\ \leftrightarrow\ \mathbf{B}_{\beta}^{\alpha}=\Theta\cdot\mathbf{B}_{q}^{d}\cdot\Theta^{-1}$$

A3.1 Components $\Theta^{-1}\cdot d\Theta/dt$ i $(d\Theta/dt)\cdot\Theta^{-1}$ calculations

On the base definition of transformation Θ (A2) we do have:

$$\frac{d\Theta}{dt}=\omega_S\begin{bmatrix}-\sin\omega_S t & -\cos\omega_S t\\ \cos\omega_S t & -\sin\omega_S t\end{bmatrix}$$

Considering Θ^{-1} matrix, one can write:

$$\Theta^{-1}\cdot\frac{d\Theta}{dt}=\frac{d\Theta}{dt}\cdot\Theta^{-1}=\omega_S\cdot\begin{bmatrix}0 & -1\\ 1 & 0\end{bmatrix}\qquad\text{(A5)}$$

Transformation of the state space equations (A3), in general case is represented by quite complicated, practically not to useful expressions. Even if square matrices **A** and **B** are diagonal, but not singular, considering (A4) one can notice, that the state space equation, stationary in (*α*-*β*) coordinates, is non-stationary in (*p*-*d*) coordinates and on the contrary. Transformation Θ can be used in the most profitably way, when matrices **A** and **B** are singular, i.e. in case of symmetrical 3-phase circuits.

A3.2 Transformations of the schemes of state equations

On the base of dependencies (A3), (A4) and (A5), with assumption of the singularity of state matrices **A** and **B** this is possible to get, in simple way, the state equations in (*α*-*β*) as well as in (*p*-*q*) coordinates and on the contrary.

If we know equation in (*α*-*β*) coordinates

$$\begin{bmatrix}\frac{dX_{\alpha}}{dt}\\ \frac{dX_{\beta}}{dt}\end{bmatrix}=A\cdot\begin{bmatrix}X_{\alpha}\\ X_{\beta}\end{bmatrix}+B\cdot\begin{bmatrix}F_{\alpha}\\ F_{\beta}\end{bmatrix}$$

then

$$\begin{bmatrix}\frac{dX_{d}}{dt}\\ \frac{dX_{q}}{dt}\end{bmatrix}=\begin{bmatrix}A & \omega_S\\ -\omega_S & A\end{bmatrix}\cdot\begin{bmatrix}X_{d}\\ X_{q}\end{bmatrix}+C\cdot\begin{bmatrix}F_{d}\\ F_{q}\end{bmatrix}$$

If we know equation in (*p*-*q*) coordinates

$$\begin{bmatrix}\frac{dX_{d}}{dt}\\ \frac{dX_{q}}{dt}\end{bmatrix}=A\cdot\begin{bmatrix}X_{d}\\ X_{q}\end{bmatrix}+B\cdot\begin{bmatrix}F_{d}\\ F_{q}\end{bmatrix}$$

then

$$\begin{bmatrix}\frac{dX_{\alpha}}{dt}\\ \frac{dX_{\beta}}{dt}\end{bmatrix}=\begin{bmatrix}A & -\omega_S\\ \omega_S & A\end{bmatrix}\cdot\begin{bmatrix}X_{\alpha}\\ X_{\beta}\end{bmatrix}+\begin{bmatrix}B & 0\\ 0 & B\end{bmatrix}\cdot\begin{bmatrix}F_{\alpha}\\ F_{\beta}\end{bmatrix}$$

Above presented transformations of the state equations are illustrated by the models in Fig.A1 and Fig.A2.

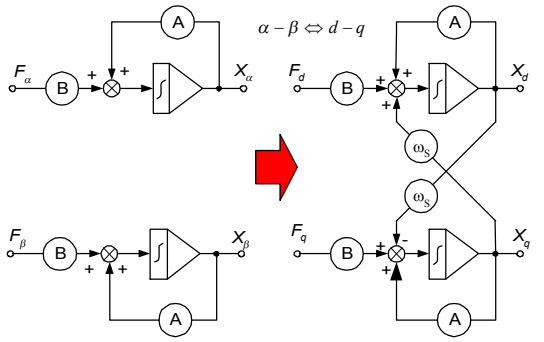

Fig.A1. Models of the state space equations in (α-β) ↔ (d-q) coordinates

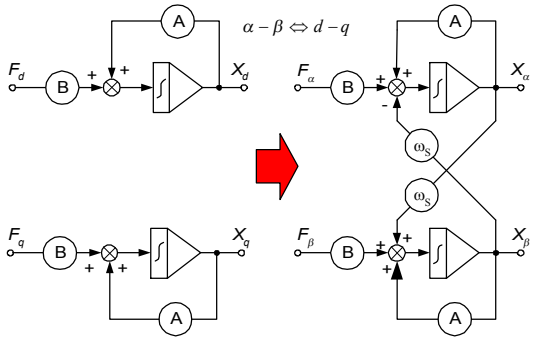

Fig.A2. Models of the state space equations in (d-q) ↔ (α-β) coordinates